

# Reanalyses for $^{42-51}\text{Ca}$ scattering on a $^{12}\text{C}$ target at 280 MeV/nucleon based on chiral $g$ folding mode with Gogny-D1S Hartree-Fock-Bogoliubov densities

Maya Takechi,<sup>1</sup> Tomotsugu Wakasa,<sup>2</sup> Shingo Tagami,<sup>2</sup> Jun Matsui,<sup>2</sup> and Masanobu Yahiro<sup>2,\*</sup>

<sup>1</sup>Niigata University, Niigata 950-2181, Japan

<sup>2</sup>Department of Physics, Kyushu University, Fukuoka 819-0395, Japan

**Background:** In the previous paper, we predicted reaction cross sections  $\sigma_R$  for  $^{40-60,62,64}\text{Ca}+^{12}\text{C}$  scattering at 280 MeV/nucleon, using the chiral  $g$ -matrix folding model with the densities calculated with the Gogny-D1S Hartree-Fock-Bogoliubov (GHFB) with and without the angular momentum projection (AMP), since Tanaka *et al.* measured interaction cross sections  $\sigma_I$  ( $\approx \sigma_R$ ) for  $^{42-51}\text{Ca}$  in RIKEN and determined neutron skin  $r_{\text{skin}}$  (RIKEN) using the optical limit of the Glauber model with the Woos-Saxon densities.

**Purpose:** Our purpose is to reanalyze the  $r_{\text{skin}}$  from the  $\sigma_I$  using the chiral  $g$ -matrix folding model. Our analysis is superior to theirs, since the chiral  $g$ -matrix folding model (the GHFB and GHFB+AMP densities) is much better than the optical limit of the Glauber model (the Woos-Saxon densities).

**Methods:** Our model is the chiral  $g$ -matrix folding model with the densities scaled from the GHFB and GHFB+AMP densities.

**Results:** We scale the GHFB and GHFB+AMP densities so that the  $\sigma_R$  of the scaled densities can agree with the central values of  $\sigma_I$  under the condition that the proton radius of the scaled proton density equals the data determined from the isotope shift based on the electron scattering. The  $r_{\text{skin}}$  thus determined are close to their results  $r_{\text{skin}}^{42-51}$  (RIKEN), except for  $^{48}\text{Ca}$ . For  $^{48}\text{Ca}$ , our value  $r_{\text{skin}}^{48}$  is  $0.105 \pm 0.06$  fm, while their value is  $r_m^{48}$  (RIKEN) =  $0.146 \pm 0.06$  fm. We then take the weighted mean and its error of our result  $r_{\text{skin}}^{48}(\sigma_I) = 0.105 \pm 0.06$  fm and the result  $r_{\text{skin}}^{48}(E1pE) = 0.17 \pm 0.03$  fm of the high-resolution  $E1$  polarizability experiment (E1pE). Our final result is  $r_{\text{skin}}^{48} = 0.157 \pm 0.027$  fm.

**Conclusion:** Our conclusion is  $r_{\text{skin}}^{48} = 0.157 \pm 0.027$  fm for  $^{48}\text{Ca}$ . For  $^{42-47,49-51}\text{Ca}$ , our results on  $r_{\text{skin}}$  are similar to theirs. Our result for  $^{48}\text{Ca}$  is related to CREX.

## I. INTRODUCTION

Very lately, Tanaka *et al.* measured interaction cross sections  $\sigma_I$  in RIKEN for  $^{42-51}\text{Ca}+^{12}\text{C}$  scattering at 280 MeV per nucleon, and determined neutron skins  $r_{\text{skin}}$  for  $^{42-51}\text{Ca}$  from the  $\sigma_I$ , using the optical limit of the Glauber model with the Woos-Saxon densities [1]. The data have high accuracy, since the average error is 1.1%. Their numerical values on matter radii  $r_m$ (RIKEN), skin values  $r_{\text{skin}}$ (RIKEN), neutron radii  $r_n$ (RIKEN), determined from  $\sigma_I$  are not presented in Ref. [1]; see Table I for their numerical values.

TABLE I. Numerical values [1] of  $r_m$ (RIKEN),  $r_n$ (RIKEN),  $r_{\text{skin}}$ (RIKEN) for  $^{42-51}\text{Ca}$ . The  $r_p$ (exp) are deduced from the electron scattering [18]. The radii are shown in units of fm. The errors include systematic errors.

A	$r_p$ (exp)	$r_m$ (RIKEN)	$r_n$ (RIKEN)	$r_{\text{skin}}$ (RIKEN)
42	$3.411 \pm 0.003$	$3.437 \pm 0.030$	$3.46 \pm 0.06$	$0.049 \pm 0.06$
43	$3.397 \pm 0.003$	$3.453 \pm 0.029$	$3.50 \pm 0.05$	$0.103 \pm 0.05$
44	$3.424 \pm 0.003$	$3.492 \pm 0.030$	$3.55 \pm 0.05$	$0.125 \pm 0.05$
45	$3.401 \pm 0.003$	$3.452 \pm 0.026$	$3.49 \pm 0.05$	$0.092 \pm 0.05$
46	$3.401 \pm 0.003$	$3.487 \pm 0.026$	$3.55 \pm 0.05$	$0.151 \pm 0.05$
47	$3.384 \pm 0.003$	$3.491 \pm 0.034$	$3.57 \pm 0.06$	$0.184 \pm 0.06$
48	$3.385 \pm 0.003$	$3.471 \pm 0.035$	$3.53 \pm 0.06$	$0.146 \pm 0.06$
49	$3.400 \pm 0.003$	$3.565 \pm 0.028$	$3.68 \pm 0.05$	$0.275 \pm 0.05$
50	$3.429 \pm 0.003$	$3.645 \pm 0.031$	$3.78 \pm 0.05$	$0.353 \pm 0.05$
51	$3.445 \pm 0.003$	$3.692 \pm 0.066$	$3.84 \pm 0.10$	$0.399 \pm 0.10$

The  $g$ -matrix folding model [2–12] is a standard way of determining matter radii  $r_m$  from measured reaction cross sections  $\sigma_R$ . In the model, the potential is obtained by folding the  $g$ -matrix with projectile and target densities.

Applying the Melbourne  $g$ -matrix folding model [3] for interaction cross sections  $\sigma_I$  of Ne isotopes and reaction cross sections  $\sigma_R$  of Mg isotopes, we deduced the  $r_m$  for Ne isotopes [10] and Mg isotopes [12], and discovered that  $^{31}\text{Ne}$  is a halo nucleus with large deformation [5].

Kohno calculated the  $g$  matrix for the symmetric nuclear matter, using the Brueckner-Hartree-Fock method with chiral  $\text{N}^3\text{LO}$  2NFs and NNLO 3NFs [13]. He set  $c_D = -2.5$  and  $c_E = 0.25$  so that the energy per nucleon can become minimum at  $\rho = \rho_0$  [9].

\* orion093g@gmail.com

Toyokawa *et al.* localized the non-local chiral  $g$  matrix into three-range Gaussian forms by using the localization method proposed by the Melbourne group [3, 14, 15]. The resulting local  $g$  matrix is called ‘‘Kyushu  $g$ -matrix’’; see the homepage <http://www.nt.phys.kyushu-u.ac.jp/english/gmatrix.html> for Kyushu  $g$ -matrix.

The Kyushu  $g$ -matrix folding model is successful in reproducing  $d\sigma/d\Omega$  and  $A_y$  for polarized proton scattering on various targets at  $E_{\text{lab}} = 65$  MeV [7] and  $d\sigma/d\Omega$  for  ${}^4\text{He}$  scattering at  $E_{\text{lab}} = 72$  MeV per nucleon [8]. This is true for  $\sigma_R$  of  ${}^4\text{He}$  scattering in  $E_{\text{lab}} = 30 \sim 200$  MeV per nucleon [9].

In the previous paper of Ref. [16], we predicted reaction cross section  $\sigma_R$  for  ${}^{40-60,62,64}\text{Ca}$  scattering on a  ${}^{12}\text{C}$  target at 280 MeV/nucleon, using the Kyushu  $g$ -matrix folding model with the reliable densities calculated with the Gogny-D1S Hartree-Fock-Bogoliubov (GHFB) with and without the angular momentum projection (AMP), since Tanaka *et al.* measured interaction cross sections  $\sigma_I (\approx \sigma_R)$  for  ${}^{42-51}\text{Ca}$  in RIKEN. As a review article on dynamical mean field approach, it is useful to see Ref. [17].

As shown in Fig. 1, the predicted  $\sigma_R$  results reproduce the data [1] in a  $2\sigma$  level. This indicates that the Kyushu  $g$ -matrix folding model with the GHFB and GHFB+AMP densities is good.

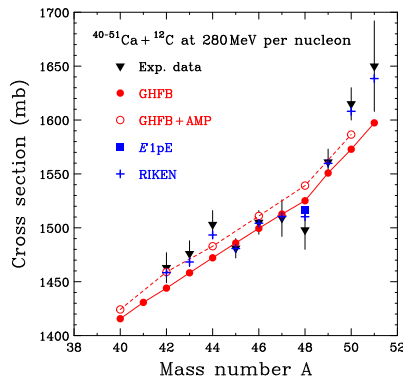


FIG. 1. Mass-number dependence of  $\sigma_R$  for  ${}^{42-51}\text{Ca}+{}^{12}\text{C}$  scattering at 280 MeV per nucleon. The folding-model results with GHFB and GHFB+AMP densities are denoted by open and closed circles, respectively. The  $\sigma_R(E1pE)$  for  ${}^{48}\text{Ca}$  is shown by squares; see Sec. III B for the definition of  $\sigma_R(E1pE)$ . We scale the proton and neutron densities calculated with GHFB and GHFB+AMP so as to  $r_p(\text{scaling}) = r_p(\text{exp})$  and  $r_n(\text{scaling}) = r_n(\text{RIKEN})$ . The results  $\sigma_R(\text{RIKEN})$  of the folding model with the scaled densities are shown by symbol ‘‘+’’; see Tabel I for  $r_p(\text{exp})$  and  $r_n(\text{RIKEN})$ . The scaling equation is shown in Sec. II C. Data on  $\sigma_I$  are taken from Ref. [1] for  ${}^{42-51}\text{Ca}$ .

Our purpose is to redetermine the  $r_{\text{skin}}$  from the  $\sigma_I$  with the Kyushu (chiral)  $g$ -matrix folding model. The Kyushu  $g$ -matrix folding model (the GHFB and GHFB+AMP densities) is much better than the optical limit of the Glauber model (the

Woos-Saxon densities).

We scale the GHFB and GHFB+AMP densities so that the  $\sigma_R$  of the scaled densities can agree with the central values of  $\sigma_I$  under the condition that the proton radius of the scaled proton density equals the data [18] determined from the isotope shift based on the electron scattering.

We explain our model in Sec. II and our results in Sec. III. Section IV is for discussions. Section V is devoted to a summary.

## II. MODEL

### A. Folding model

In the  $g$ -matrix folding model, the potential  $U(\mathbf{R})$  consists of the direct and the exchange part defined in Ref. [10]:

$$U^{\text{DR}}(\mathbf{R}) = \sum_{\mu, \nu} \int \rho_P^\mu(\mathbf{r}_P) \rho_T^\nu(\mathbf{r}_T) g_{\mu\nu}^{\text{DR}}(s) d\mathbf{r}_P d\mathbf{r}_T, \quad (1)$$

$$U^{\text{EX}}(\mathbf{R}) = \sum_{\mu, \nu} \int \rho_P^\mu(\mathbf{r}_P, \mathbf{r}_P - \mathbf{s}) \rho_T^\nu(\mathbf{r}_T, \mathbf{r}_T + \mathbf{s}) \times g_{\mu\nu}^{\text{EX}}(s) \exp[-i\mathbf{K}(\mathbf{R}) \cdot \mathbf{s}/M] d\mathbf{r}_P d\mathbf{r}_T, \quad (2)$$

where  $\mathbf{s} = \mathbf{r}_P - \mathbf{r}_T + \mathbf{R}$  for the coordinate  $\mathbf{R}$  between a projectile (P) and a target (T). The coordinate  $\mathbf{r}_P$  ( $\mathbf{r}_T$ ) denotes the location for the interacting nucleon measured from the center-of-mass of P (T). Each of  $\mu$  and  $\nu$  stands for the  $z$ -component of isospin;  $1/2$  means neutron and  $-1/2$  does proton. The original form of  $U^{\text{EX}}$  is a non-local function of  $\mathbf{R}$ , but it has been localized in Eq. (2) with the local semi-classical approximation [2] in which P is assumed to propagate as a plane wave with the local momentum  $\hbar\mathbf{K}(\mathbf{R})$  within a short range of the nucleon-nucleon interaction, where  $M = AA_T/(A + A_T)$  for the mass number  $A$  ( $A_T$ ) of P (T). The validity of this localization is shown in Ref. [19].

The direct and exchange parts,  $g_{\mu\nu}^{\text{DR}}$  and  $g_{\mu\nu}^{\text{EX}}$ , of the  $g$  matrix are described by

$$g_{\mu\nu}^{\text{DR}}(s) = \begin{cases} \frac{1}{4} \sum_S \hat{S}^2 t_{\mu\nu}^{S1}(s) & ; \text{ for } \mu + \nu = \pm 1 \\ \frac{1}{8} \sum_{S,T} \hat{S}^2 t_{\mu\nu}^{ST}(s), & ; \text{ for } \mu + \nu = 0 \end{cases} \quad (3)$$

$$g_{\mu\nu}^{\text{EX}}(s) = \begin{cases} \frac{1}{4} \sum_S (-1)^{S+1} \hat{S}^2 t_{\mu\nu}^{S1}(s) & ; \text{ for } \mu + \nu = \pm 1 \\ \frac{1}{8} \sum_{S,T} (-1)^{S+T} \hat{S}^2 t_{\mu\nu}^{ST}(s) & ; \text{ for } \mu + \nu = 0 \end{cases} \quad (4)$$

where the  $g_{\mu\nu}^{ST}$  are the spin-isospin ( $S$ - $T$ ) components of the  $g$ -matrix interaction and  $\hat{S} = \sqrt{2S+1}$ . As a way of the center-of-mass (cm) corrections in the proton and neutron densities, we take the method of Ref. [10], since it is very

simple. As for  $^{12}\text{C}$ , we use a phenomenological density of Ref. [20]. As for Ca isotopes, we take the densities scaled from the GHFB and GHFB+AMP densities.

### B. GHFB and GHFB+AMP

In GHFB+AMP, the total wave function  $|\Psi_M^I\rangle$  with the AMP is defined by

$$|\Psi_M^I\rangle = \sum_{K,n=1}^{N+1} g_{Kn}^I \hat{P}_{MK}^I |\Phi_n\rangle, \quad (5)$$

where  $\hat{P}_{MK}^I$  is the angular-momentum-projector and the  $|\Phi_n\rangle$  for  $n = 1, 2, \dots, N+1$  are mean-field (GHFB) states, where  $N$  is the number of the states. The coefficients  $g_{Kn}^I$  are determined by solving the following Hill-Wheeler equation,

$$\sum_{K'n'} \mathcal{H}_{Kn,K'n'}^I g_{K'n'}^I = E_I \sum_{K'n'} \mathcal{N}_{Kn,K'n'}^I g_{K'n'}^I, \quad (6)$$

with the Hamiltonian and norm kernels defined by

$$\left\{ \begin{array}{c} \mathcal{H}_{Kn,K'n'}^I \\ \mathcal{N}_{Kn,K'n'}^I \end{array} \right\} = \langle \Phi_n | \left\{ \begin{array}{c} \hat{H} \\ 1 \end{array} \right\} \hat{P}_{K'n'}^I | \Phi_{n'} \rangle. \quad (7)$$

For odd nuclei, we have to put a quasi-particle in a level, but the number of the blocking states are quite large. It is difficult to solve the Hill-Wheeler equation with large  $N$ . Furthermore, we have to confirm that the resulting  $|\Psi_M^I\rangle$  converges with respect to increasing  $N$  for any set of two deformations  $\beta$  and  $\gamma$ . This procedure is quite time-consuming. For this reason, it is not feasible to perform the AMP for odd nuclei. As for GHFB, we consider the one-quasiparticle state that yields the lowest energy, so that we do not have to solve the Hill-Wheeler equation. However, it is not easy to find the values of  $\beta$  and  $\gamma$  at which the energy becomes minimum in the  $\beta$ - $\gamma$  plane.

For even nuclei, there is no blocking state in the Hill-Wheeler equation. We can thus consider GHFB+AMP. However, we have to find the value of  $\beta$  at which the ground-state energy becomes minimum. In this step, the AMP has to be performed for any  $\beta$ , so that the Hill-Wheeler calculation is still heavy. In fact, the AMP is not taken for most of mean field calculations; see for example Ref. [21]. The reason why we do not take into account  $\gamma$  deformation is that the deformation does not affect  $\sigma_R$  [10].

### C. The scaling of the GHFB and GHFB+AMP densities

We explain the scaling of original density  $\rho(\mathbf{r})_{\text{original}}$ . We can obtain the scaled density  $\rho_{\text{scaling}}(\mathbf{r})$  from the original one as

$$\rho_{\text{scaling}}(\mathbf{r}) = \frac{1}{\alpha^3} \rho_{\text{original}}(\mathbf{r}/\alpha) \quad (8)$$

with a scaling factor

$$\alpha = \sqrt{\frac{\langle r^2 \rangle_{\text{scaling}}}{\langle r^2 \rangle_{\text{original}}}}. \quad (9)$$

For later convenience, we refer to the proton (neutron) radius of the scaled density as  $r_p(\text{scaling})$  ( $r_n(\text{scaling})$ ).

## III. RESULTS

### A. $^{42-51}\text{Ca}$

Table II show theoretical radii determined with GHFB and GHFB+AMP for  $^{39-64}\text{Ca}$ . Effects of the AMP are small for radii.

TABLE II. Theoretical radii for Ca isotopes. The superscript ‘‘AMP’’ stands for the results of GHFB+AMP, and no superscript corresponds to those of GHFB.

$A$	$r_n^{\text{AMP}}$	$r_p^{\text{AMP}}$	$r_m^{\text{AMP}}$	$r_{\text{skin}}^{\text{AMP}}$	$r_n$	$r_p$	$r_m$	$r_{\text{skin}}$
39					3.320	3.381	3.351	-0.061
40	3.366	3.412	3.389	-0.046	3.349	3.393	3.371	-0.044
41					3.387	3.397	3.392	-0.010
42	3.451	3.424	3.438	0.026	3.417	3.401	3.409	-0.010
43					3.448	3.405	3.428	0.043
44	3.501	3.426	3.467	0.075	3.477	3.410	3.447	0.067
45					3.504	3.414	3.465	0.090
46	3.555	3.436	3.504	0.118	3.530	3.420	3.483	0.110
47					3.554	3.424	3.499	0.130
48	3.604	3.445	3.539	0.159	3.576	3.428	3.515	0.148
49					3.621	3.440	3.548	0.181
50	3.687	3.469	3.601	0.218	3.658	3.452	3.577	0.206
51					3.698	3.462	3.607	0.236
52	3.760	3.490	3.659	0.270	3.734	3.475	3.659	0.270
53					3.779	3.486	3.671	0.293
54	3.840	3.524	3.726	0.316	3.817	3.507	3.705	0.310
55					3.856	3.524	3.739	0.332
56	3.913	3.557	3.790	0.357	3.891	3.541	3.770	0.350
57					3.928	3.557	3.802	0.370
58	3.977	3.588	3.847	0.389	3.958	3.575	3.830	0.383
59					3.995	3.593	3.863	0.402
60	4.043	3.611	3.904	0.432	4.020	3.608	3.888	0.412
62	4.106	3.637	3.961	0.469	4.067	3.628	3.931	0.439
64	4.153	3.658	4.005	0.494	4.113	3.648	3.974	0.465

As proton and neutron densities, we use GHFB for odd nuclei and GHFB+AMP for even nuclei, and scale the GHFB and GHFB+AMP densities so that the scaled proton and neutron radii may agree with  $r_p(\text{exp})$  [18] of electron scattering and  $r_n(\text{RIKEN})$ , respectively; namely  $r_p(\text{scaling}) = r_p(\text{exp})$  and  $r_n(\text{scaling}) = r_n(\text{RIKEN})$ .

Figure 1 shows mass-number ( $A$ ) dependence of  $\sigma_R$  for  $^{42-51}\text{Ca}$  scattering on a  $^{12}\text{C}$  target at 280 MeV per nucleon.

The folding model with GHFB and GHFB+AMP densities (open and closed circles) reproduce the data [1] in a  $2\sigma$  level, indicating that the folding model is reliable. This allows us to scale the proton and neutron densities calculated with GHFB and GHFB+AMP so as to  $r_p(\text{scaling}) = r_p(\text{exp})$  and  $r_n(\text{scaling}) = r_n(\text{RIKEN})$ . The folding-model results (+) with the scaled densities mentioned above slightly deviate the central values of  $\sigma_I$ . The small deviation comes from the method taken.

Now we redetermine  $r_n$ ,  $r_m$  and  $r_{\text{skin}}$  from the data [1] on  $\sigma_I$ , using  $r_p(\text{exp})$  [18] of electron scattering. For this purpose, we scale the proton and neutron densities of GHFB and GHFB+AMP so that the  $\sigma_R$  calculated with the scaled densities may agree with the central values of  $\sigma_I$  under the condition that  $r_p(\text{scaling}) = r_p(\text{exp})$ . The resulting values  $r_n(\sigma_I)$  and the  $r_p(\text{exp})$  yield  $r_m(\sigma_I)$  and  $r_{\text{skin}}(\sigma_I)$ . Our results are tabulated in Table III.

TABLE III. Our values on  $r_p(\text{exp})$ ,  $r_m(\sigma_I)$ ,  $r_n(\sigma_I)$ ,  $r_{\text{skin}}(\sigma_I)$  for  $^{42-51}\text{Ca}$ . The  $r_p(\text{exp})$  are deduced from the charge radii [18]. The errors are taken from the original data of Ref. [1].

A	$r_p(\text{exp})$ fm	$r_m(\sigma_I)$ fm	$r_n(\sigma_I)$ fm	$r_{\text{skin}}(\sigma_I)$ fm
42	$3.411 \pm 0.003$	$3.446 \pm 0.030$	$3.477 \pm 0.06$	$0.066 \pm 0.06$
43	$3.397 \pm 0.003$	$3.468 \pm 0.029$	$3.529 \pm 0.05$	$0.132 \pm 0.05$
44	$3.424 \pm 0.003$	$3.511 \pm 0.030$	$3.582 \pm 0.05$	$0.158 \pm 0.05$
45	$3.401 \pm 0.003$	$3.452 \pm 0.026$	$3.493 \pm 0.05$	$0.092 \pm 0.05$
46	$3.401 \pm 0.003$	$3.489 \pm 0.026$	$3.555 \pm 0.05$	$0.154 \pm 0.05$
47	$3.384 \pm 0.003$	$3.488 \pm 0.034$	$3.563 \pm 0.06$	$0.179 \pm 0.06$
48	$3.385 \pm 0.003$	$3.447 \pm 0.035$	$3.490 \pm 0.06$	$0.105 \pm 0.06$
49	$3.400 \pm 0.003$	$3.568 \pm 0.028$	$3.679 \pm 0.05$	$0.279 \pm 0.05$
50	$3.429 \pm 0.003$	$3.658 \pm 0.031$	$3.803 \pm 0.05$	$0.374 \pm 0.05$
51	$3.445 \pm 0.003$	$3.713 \pm 0.066$	$3.877 \pm 0.10$	$0.432 \pm 0.10$

## B. $^{48}\text{Ca}$

We consider  $r_{\text{skin}}^{48}$ , since  $r_{\text{skin}}^{48}$  is related to the slope parameter  $L$  in neutron matter [22]. As a measurement on skin  $r_{\text{skin}}^{48}$ , the high-resolution  $E1$  polarizability experiment ( $E1pE$ ) was made for  $^{48}\text{Ca}$  [23] in RCNP. The result is

$$r_{\text{skin}}^{48}(E1pE) = 0.17 \pm 0.03 = 0.14 - 0.20 \text{ fm}. \quad (10)$$

For  $r_{\text{skin}}^{48}$ , the measurement is most reliable in the present stage. The central value 0.17 fm of Eq. (10) yields matter radius  $r_m(E1pE) = 3.485$  fm and neutron radius  $r_n(E1pE) = 3.555$  fm from proton radius  $r_p(\text{exp}) = 3.385$  fm evaluated with the isotope shift method based on the electron scattering [18]. We then scale the proton and neutron densities calculated with GHFB+AMP so as to reproduce  $r_p(\text{exp})$  and  $r_n(E1pE)$ . In Fig. 1, the  $\sigma_R(E1pE)$  calculated with the scaled densities is near the upper bound of  $\sigma_I$ .

We take the weighted mean and its error for  $r_{\text{skin}}^{48}(E1pE) = 0.17 \pm 0.03$  fm and our result  $r_{\text{skin}}(\sigma_I) = 0.105 \pm 0.06$  fm.

The final result is

$$r_{\text{skin}} = 0.157 \pm 0.027 \text{ fm}. \quad (11)$$

Our final result is shown in Fig. 2, together with  $r_{\text{skin}}^{48}(E1pE) = 0.17 \pm 0.03$  fm and our result  $r_{\text{skin}}(\sigma_I) = 0.105 \pm 0.06$  fm.

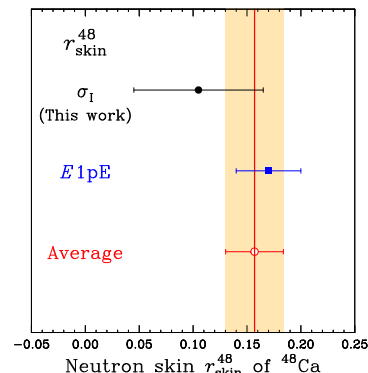


FIG. 2.  $r_{\text{skin}}^{48}(\sigma_I)$ ,  $r_{\text{skin}}^{48}(E1pE)$ , the weighted mean and its error for the two values.

As an *ab initio* method for Ca isotopes, we should consider the coupled-cluster method [24, 25] with chiral interaction. Chiral interactions were constructed by two groups [26–28]. The coupled-cluster result [24]

$$r_{\text{skin}}^{48}(\text{CC}) = 0.12 - 0.15 \text{ fm} \quad (12)$$

is consistent with our final result of Eq. (11).

## IV. DISCUSSIONS

Mass-number dependence  $A$  of  $\sigma_I$  has a kink at  $A = 48$ . The data on  $\alpha \equiv r_m E_B / (A\hbar c)$  hardly depend on  $A$ , as shown in Table IV; note that  $E_B$  is the binding energy of a nucleus. Here, the central values of data on  $r_m$  and  $E_B$  are taken from Refs. [1, 29]. In fact, the deviation of  $\alpha$  is much smaller than the average value; namely,

$$\alpha = 0.1535(9) \quad (13)$$

for  $^{42-51}\text{Ca}$ . This indicates that  $r_m$  is in inverse proportion to  $E_B/A$  as an experimental result.

TABLE IV. Numerical values of  $\alpha \equiv r_m E_B / (A\hbar c)$ ,  $r_m(\sigma_I)$ ,  $E_B/A$  for  $^{42-51}\text{Ca}$ . The data  $r_m(\sigma_I)$  on  $r_m$  are taken from Ref. [1], and the data on  $E_B/A$  are from Ref. [29].

A	$r_m(\text{RIKEN})$ fm	$E_B/A$ MeV	$\alpha$
42	3.437	8.616563	0.1501
43	3.453	8.600663	0.1505
44	3.492	8.658175	0.1532
45	3.452	8.630545	0.1510
46	3.487	8.66898	0.1532
47	3.491	8.63935	0.1528
48	3.471	8.666686	0.1524
49	3.565	8.594844	0.1553
50	3.645	8.55016	0.1579
51	3.692	8.476913	0.1586

For  $r_{\text{skin}}^{48}$ , the difference between  $\sigma_R(E1\text{pE})$  and the central value of  $\sigma_I$  may come from that between reaction cross section and interaction cross section, i.e.,  $\sigma_R(E1\text{pE}) - \sigma_I = 18.5$  mb. We assume that the difference  $\sigma_R(E1\text{pE}) - \sigma_I = 18.5$  mb for  $^{48}\text{Ca}$  is the same as for  $^{42-51}\text{Ca}$ . The estimated  $\sigma_R$  is  $\sigma_I + 18.5$  mb in which the error on the estimated  $\sigma_R$  is 2.5% larger than the error 1.1% on  $\sigma_I$ ; as a good experiment on  $\sigma_R$ , we can consider  $^9\text{Be}$ ,  $^{12}\text{C}$ ,  $^{27}\text{Al} + ^{12}\text{C}$  scattering of Ref. [30] and the error is 2 ~ 3%. The figure 3 is shown below.

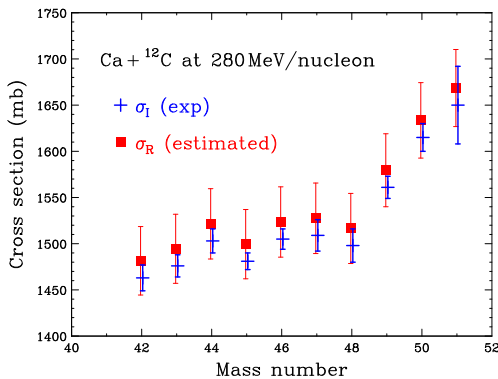


FIG. 3. Mass-number dependence of  $\sigma_R$  and  $\sigma_I$  for  $^{42-51}\text{Ca} + ^{12}\text{C}$  scattering at 280 MeV per nucleon. The estimated  $\sigma_R$  are shown by squares, while the data on  $\sigma_I$  are by the symbol “+”. Data on  $\sigma_I$  are taken from Ref. [1] for  $^{42-51}\text{Ca}$ .

Now we assume that  $\sigma_R = \sigma_I(\text{RIKEN}) + 18.5$  mb as the data for  $^{42-51}\text{Ca}$ . Using the estimated  $\sigma_R$  instead of  $\sigma_I$ , we take the same procedure in order to obtain  $r_{\text{skin}}(\sigma_R)$ .

As shown in Table V, the resulting  $r_{\text{skin}}(\sigma_R)$  is almost the same as the  $r_{\text{skin}}(\text{RIKEN})$  of Ref. [1], except for  $^{48}\text{Ca}$ . As for  $^{48}\text{Ca}$ , our estimates value  $0.170 \pm 0.06$  fm agrees with  $r_{\text{skin}}^{48}(E1\text{pE}) = 0.17 \pm 0.03$  fm of Ref. [23].

TABLE V. Numerical values of estimated  $r_{\text{skin}}(\sigma_R)$ ,  $r_{\text{skin}}(\text{RIKEN})$  [1] for  $^{42-51}\text{Ca}$ . The skins are shown in units of fm.

A	$r_{\text{skin}}(\sigma_R)$	$r_{\text{skin}}(\text{RIKEN})$
42	$0.049 \pm 0.06$	$0.049 \pm 0.06$
43	$0.104 \pm 0.05$	$0.103 \pm 0.05$
44	$0.124 \pm 0.05$	$0.125 \pm 0.05$
45	$0.091 \pm 0.05$	$0.092 \pm 0.05$
46	$0.151 \pm 0.05$	$0.151 \pm 0.05$
47	$0.184 \pm 0.06$	$0.184 \pm 0.06$
48	$0.170 \pm 0.06$	$0.146 \pm 0.06$
49	$0.275 \pm 0.05$	$0.275 \pm 0.05$
50	$0.353 \pm 0.05$	$0.353 \pm 0.05$
51	$0.398 \pm 0.10$	$0.399 \pm 0.10$

## V. SUMMARY

Recently, Tanaka *et al.* measured  $\sigma_I$  in RIKEN for  $^{42-51}\text{Ca} + ^{12}\text{C}$  scattering at 280 MeV per nucleon, and determined neutron skins  $r_{\text{skin}}$  for  $^{42-51}\text{Ca}$  from the  $\sigma_I$ , using the optical limit of the Glauber model with the Woods-Saxon densities [1]. We redetermine  $r_{\text{skin}}$ ,  $r_m$ ,  $r_n$  for  $^{42-51}\text{Ca}$ , using the Kyushu folding model with the proton and neutron densities scaled from the GHFB and GHFB+AMP densities.

The  $\sigma_R$  calculated with the GHFB and GHFB+AMP densities almost reproduce the data [1] on  $\sigma_I$ . This allows us to determine  $r_{\text{skin}}$  from the central values of  $\sigma_I$  by scaling the proton and neutron densities. The  $r_{\text{skin}}$  thus determined are close to the original ones of Ref. [1], except for  $r_{\text{skin}}^{48}$ ; see Table I for the original values and Table III for ours. The  $r_{\text{skin}}$  thus determined are close to the original results  $r_{\text{skin}}^{42-51}(\text{RIKEN})$ , except for  $^{48}\text{Ca}$ . Our experimental values on  $r_m$ ,  $r_n$ ,  $r_{\text{skin}}$  for  $^{42-51}\text{Ca}$  are summarized in Table III.

For  $^{48}\text{Ca}$ , our value is  $r_{\text{skin}}^{48}(\sigma_I) = 0.105 \pm 0.06$  fm, while Birkhan *et al.* determined  $r_{\text{skin}}^{48}(E1\text{pE}) = 0.17 \pm 0.03$  fm [23] from the high-resolution  $E1$  polarizability experiment (E1pE). We then take the weighted mean and its error for the two values. The resulting value  $r_{\text{skin}}^{48} = 0.157 \pm 0.027$  fm is our final value for  $^{48}\text{Ca}$ . The value is related to CREX that is ongoing.

## ACKNOWLEDGEMENTS

We thank Dr. Tanaka and Prof. Fukuda for providing the data and helpful comments. M. Y. thanks Dr. M. Toyokawa heartily.

- 
- [1] M. Tanaka *et al.*, Phys. Rev. Lett. **124**, 102501 (2020). [arXiv:1911.05262 [nucl-ex]].
- [2] F. A. Brieva and J. R. Rook, Nucl. Phys. A **291**, 299 (1977); *ibid.* 291, 317 (1977); *ibid.* 297, 206 (1978).
- [3] K. Amos, P. J. Dortmans, H. V. von Geramb, S. Karataglidis, and J. Raynal, in *Advances in Nuclear Physics*, edited by J. W. Negele and E. Vogt (Plenum, New York, 2000) Vol. 25, p. 275.
- [4] T. Furumoto, Y. Sakuragi, and Y. Yamamoto, Phys. Rev. C **78**, 044610 (2008).
- [5] K. Minomo, T. Sumi, M. Kimura, K. Ogata, Y. R. Shimizu and M. Yahiro, Phys. Rev. Lett. **108**, 052503 (2012), [arXiv:1110.3867 [nucl-th]].
- [6] M. Toyokawa, K. Minomo and M. Yahiro, Phys. Rev. C **88**, no. 5, 054602 (2013), [arXiv:1304.7884 [nucl-th]].
- [7] M. Toyokawa, K. Minomo, M. Kohno and M. Yahiro, J. Phys. G **42**, no. 2, 025104 (2015), Erratum: [J. Phys. G **44**, no. 7, 079502 (2017)] [arXiv:1404.6895 [nucl-th]].
- [8] M. Toyokawa, M. Yahiro, T. Matsumoto, K. Minomo, K. Ogata and M. Kohno, Phys. Rev. C **92**, no. 2, 024618 (2015), Erratum: [Phys. Rev. C **96**, no. 5, 059905 (2017)], [arXiv:1507.02807 [nucl-th]].
- [9] M. Toyokawa, M. Yahiro, T. Matsumoto and M. Kohno, PTEP **2018**, 023D03 (2018), [arXiv:1712.07033 [nucl-th]]. See <http://www.nt.phys.kyushu-u.ac.jp/english/gmatrix.html> for Kyushu *g*-matrix.
- [10] T. Sumi, K. Minomo, S. Tagami, M. Kimura, T. Matsumoto, K. Ogata, Y. R. Shimizu and M. Yahiro, Phys. Rev. C **85**, 064613 (2012), [arXiv:1201.2497 [nucl-th]].
- [11] K. Egashira, K. Minomo, M. Toyokawa, T. Matsumoto and M. Yahiro, Phys. Rev. C **89**, 064611 (2014). [arXiv:1404.2735 [nucl-th]].
- [12] S. Watanabe *et al.*, Phys. Rev. C **89**, no. 4, 044610 (2014), [arXiv:1404.2373 [nucl-th]].
- [13] M. Kohno, Phys. Rev. C **88**, 064005 (2013).  
M. Kohno, Phys. Rev. C **96**, 059903(E) (2017).
- [14] H. V. von Geramb, K. Amos, L. Berge, S. Bräutigam, H. Kohlhoff and A. Ingemarsson, Phys. Rev. C **44**, 73 (1991).
- [15] P. J. Dortmans and K. Amos, Phys. Rev. C **49**, 1309 (1994).
- [16] S. Tagami, M. Tanaka, M. Takechi, M. Fukuda and M. Yahiro, Phys. Rev. C **101**, no. 1, 014620 (2020), [arXiv:1911.05417 [nucl-th]].
- [17] C. Simenel, Lect. Notes Phys. **875**, 95-145 (2014) doi:10.1007/978-3-319-01077-9\_4 [arXiv:1211.2387 [nucl-th]].
- [18] I. Angeli and K. P. Marinova, Atom. Data Nucl. Data Tabel. **99**, 69 (2013).
- [19] K. Minomo, K. Ogata, M. Kohno, Y. R. Shimizu, and M. Yahiro, J. Phys. G **37**, 085011 (2010) [arXiv:0911.1184 [nucl-th]].
- [20] H. de Vries, C. W. de Jager, and C. de Vries, At. Data Nucl. Data Tables **36**, 495 (1987).
- [21] S. Hilaire and M. Girod, Hartree-Fock-Bogoliubov results based on the Gogny force; <http://www-phynu.cea.fr/science-en-ligne/carte-potentiels-microscopiques/carte-potentiel-nucleaire-eng.htm>.
- [22] S. Tagami, N. Yasutake, M. Fukuda and M. Yahiro, [arXiv:2003.06168 [nucl-th]].
- [23] J. Birkhan *et al.*, Phys. Rev. Lett. **118**, no. 25, 252501 (2017), [arXiv:1611.07072 [nucl-ex]].
- [24] G. Hagen *et al.*, Nature Phys. **12**, 186 (2015), [arXiv:1509.07169 [nucl-th]].
- [25] G. Hagen, T. Papenbrock, M. Hjorth-Jensen and D. J. Dean, Rept. Prog. Phys. **77**, 096302 (2014), [arXiv:1312.7872 [nucl-th]].
- [26] S. Weinberg, Nucl. Phys. B **363**, 3 (1991).
- [27] E. Epelbaum, H. W. Hammer and U. G. Meissner, Rev. Mod. Phys. **81**, 1773 (2009). [arXiv:0811.1338 [nucl-th]].
- [28] R. Machleidt and D. R. Entem, Phys. Rept. **503**, 1 (2011), [arXiv:1105.2919 [nucl-th]].
- [29] the National Nuclear Data Center, NuDat 2.8; <https://www.nndc.bnl.gov/nudat2/>.
- [30] M. Takechi, M. Fukuda, M. Mihara, K. Tanaka, T. Chinda, T. Matsumasa, M. Nishimoto, R. Matsumiya, Y. Nakashima and H. Matsubara, *et al.* Phys. Rev. C **79** (2009), 061601 doi:10.1103/PhysRevC.79.061601